

Supporting Information

High spin to charge conversion efficiency in electron beam evaporated topological insulator Bi_2Se_3

Braj Bhusan Singh^{1*}, Sukanta Kumar Jena¹, Manisha Samanta², Kanishka Biswas², and Subhankar Bedanta^{1*}

¹Laboratory for Nanomagnetism and Magnetic Materials (LNMM), School of Physical Sciences,

National Institute of Science Education and Research (NISER), HBNI, Jatni-752050, India

²New Chemistry Unit, Jawaharlal Nehru Centre for Advanced Scientific Research, Jakkur, Bangalore, 560064, India

Corresponding Authors

Braj Bhusan Singh, email: brajbhusan@niser.ac.in

Subhankar Bedanta, email: sbedanta@niser.ac.in

Figure S1 and S2 show angle dependent V_{sym} (V_{asym}) components for the samples BB3-BB10. Experimental data is represented by solid circles. The data was fitted using equations (2) and (3), which is represented by solid lines.

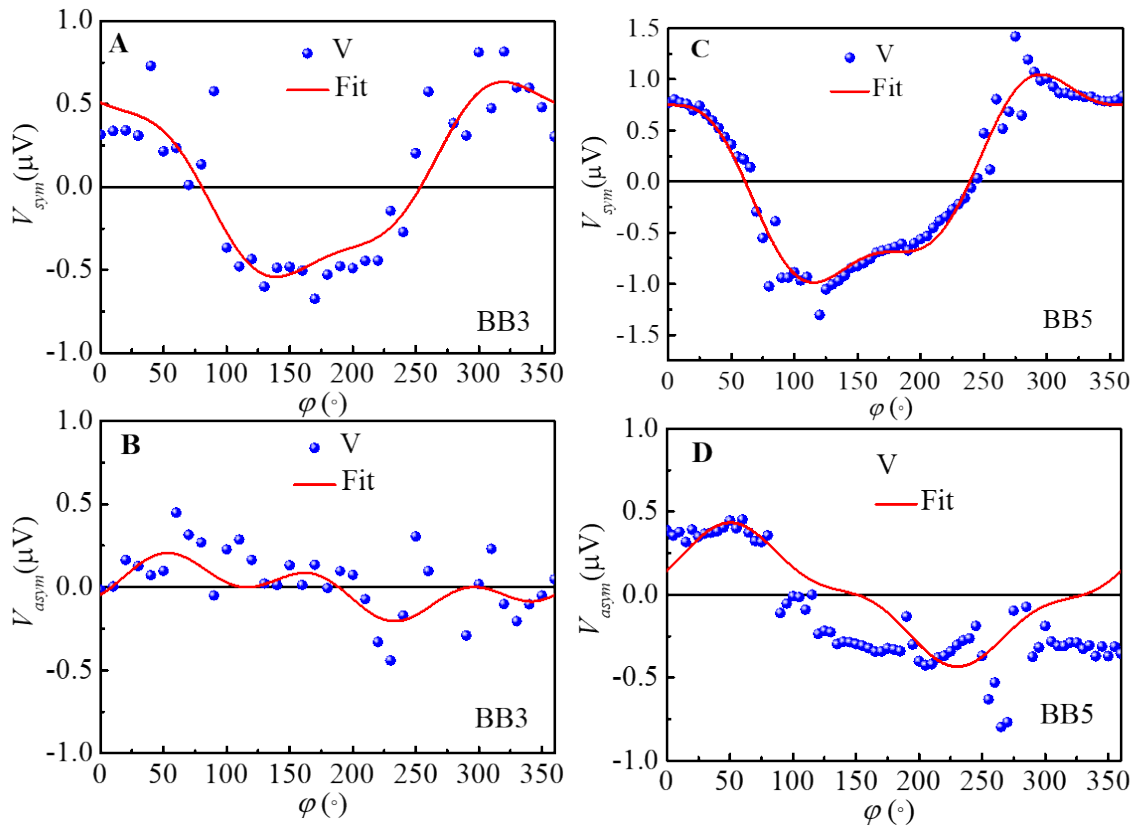


Fig. S1 A (B) and C (D) presents the angle dependent V_{sym} (V_{asym}) components for samples BB3 and BB4, respectively. Circles and solid lines are experimental data and best fits using equation (2) and (3), respectively.

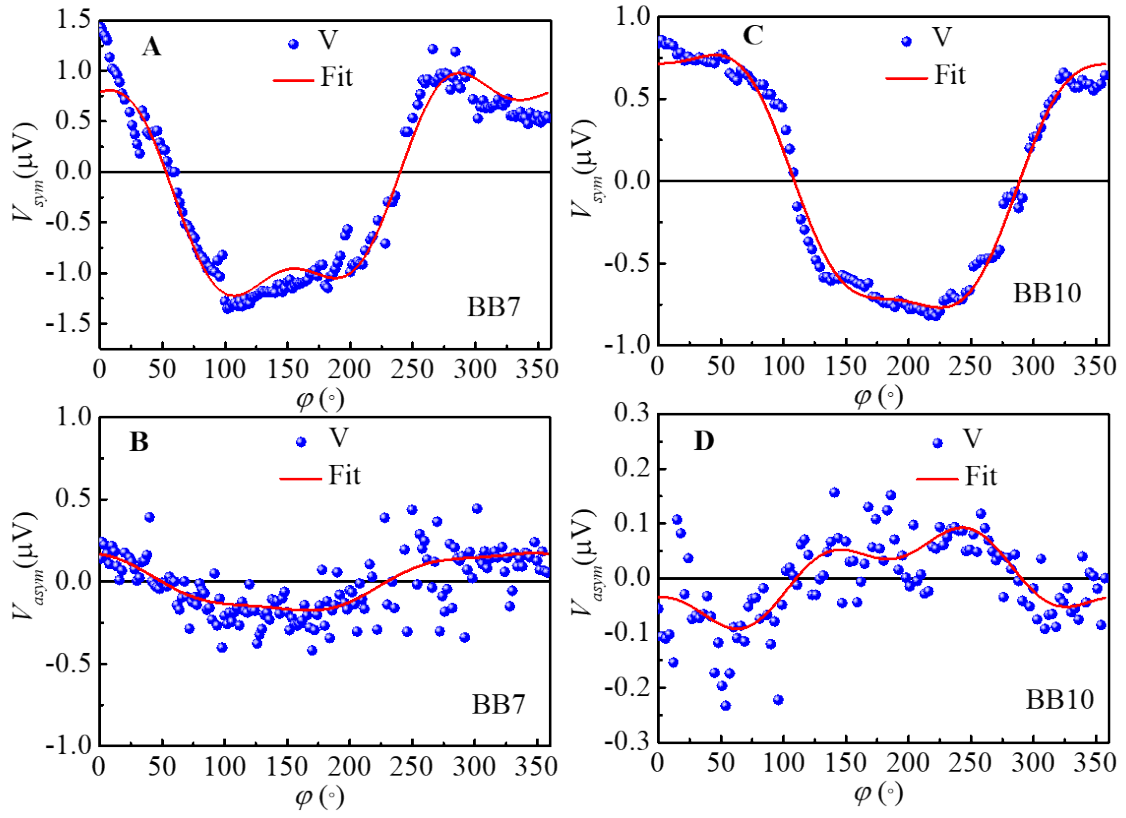


Fig. S2 A (B) and C (D) presents the angle dependent V_{sym} . (V_{asym}) components for samples BB7 and BB10, respectively. Circles and solid lines are experimental data and best fits using equation (2) and (3), respectively.

Figure S3 shows frequency dependent resonance field H_{res} and line width ΔH for the sample Si/native SiO_2 /CoFeB (5 nm)/ TaO_x (2 nm). Open symbols are experimental data and solid lines are the best fits using equation (4) and (5). The value of damping constant (α_{CoFeB}) for CoFeB single layer is found to be 0.0066 ± 0.0001 .

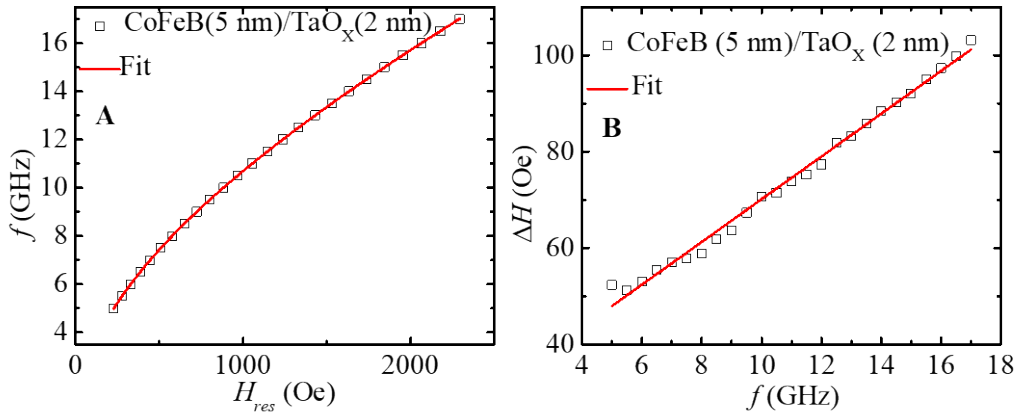


Fig. S3 Frequency (f) dependence of A. H_{res} and B. ΔH for CoFeB (5 nm)/TaO_x (2 nm). Solid symbols are experimental data, while solid lines are best fit using equation (4) and (5) in A and B, respectively.

In order to understand the two magnon scattering (TMS) contribution in our samples, if any, in the linewidth (ΔH), we have performed polar angle (θ_p) dependence FMR measurements at excitation frequency $f = 6.5$ GHz. FMR spectra was fitted to Lorentzian function to evaluate

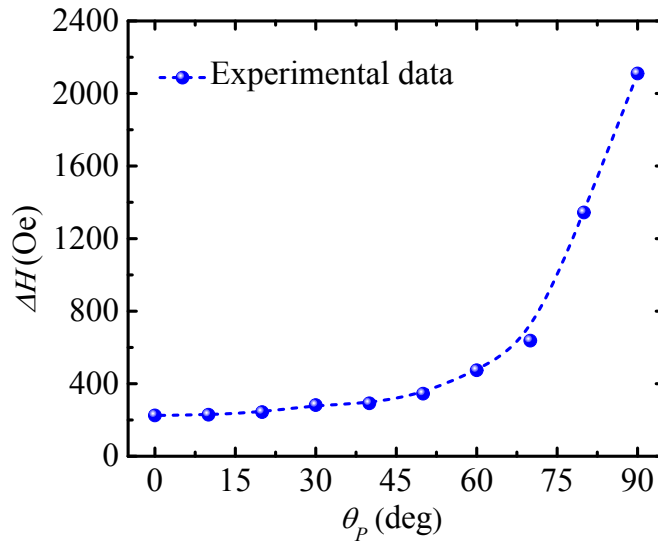


Fig. S4 Polar angle (θ_p) dependence of line width (ΔH) measured at $f = 6.5$ GHz for the sample BB20.

ΔH . Figure S4 shows the ΔH versus θ_p data. It is observed that ΔH is increasing up to $\theta_p = 90^\circ$ monotonically. It is noted that $\theta_p = 90^\circ$ means magnetic field is applied perpendicular to the

sample plane. It is well known that at $\theta_p = 90^\circ$ TMS will be zero (1, 2). Therefore, if there is any contribution of TMS, the value of ΔH should decrease in comparison to in-plane magnetic field ($\theta_p = 0^\circ$). However, in our sample it is monotonically increasing with θ_p . Therefore, it is concluded that TMS is not having any measurable contribution in the ΔH and hence in effective damping constant (α_{eff}). It has been reported that TMS contribution is only significant when thickness of CoFeB is 1-2 nm (2). It is diminished for the 4 nm thick CoFeB layer. Therefore, it may be the reason in our case since our samples are having 5 nm thick CoFeB.

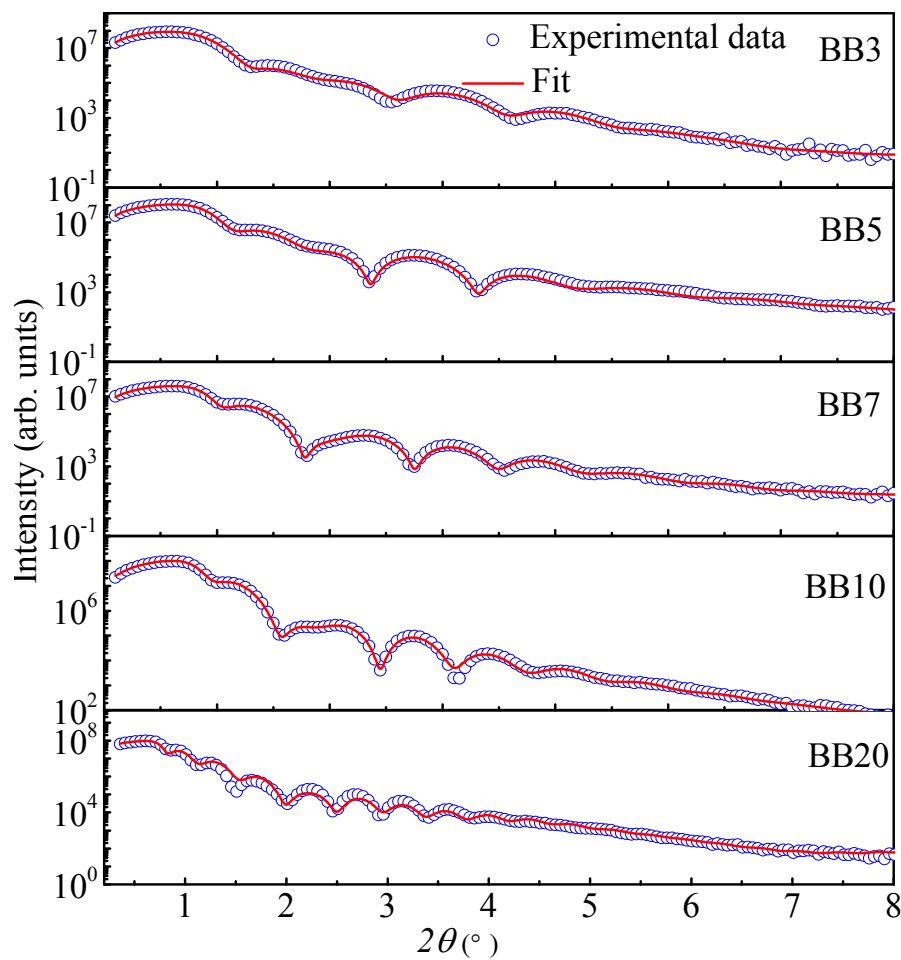


Fig. S5 X-ray reflectivity of the samples BB3-BB20. Circles and solid lines are experimental data and best fits, respectively.

In order to understand the interface quality, we have performed x-ray reflectivity (XRR) measurements, which are shown in Fig. S5. Experimental data were fitted using X'Pert

reflectivity software, which is shown by solid lines. From the best fits, we have observed Bi_2Se_3 -CoFeB interface roughness 0.7 ± 0.02 , 0.8 ± 0.02 , 1.2 ± 0.03 , 1.2 ± 0.03 , and 0.8 ± 0.02 , for the samples BB3-BB20, respectively.

It is noted that thermal effects may also cause to produce a voltage due to spin Seebeck, Nernst, and anomalous Nernst effect, which may contaminate spin pumping voltage (3). In order to quantify voltages generated due to thermal effects, we have prepared two samples S1#Si/Bi₂Se₃ (10 nm)/MgO (2 nm)/CoFeB (5 nm)/TaOx (2 nm), and S2#Si/Bi₂Se₃ (10 nm)/CoFeB (5 nm)/TaOx (2 nm), where MgO is used as a barrier for spin current. If thermal effects are dominating, then one should obtain similar strength of voltage signal in both the samples. We have performed inverse spin Hall effect (ISHE) measurements on both the samples and data is shown in the Figure S6. Experimental data was fitted to equation (1) of the manuscript to obtain V_{sym} and V_{asym} components. Table S1 shows the V_{sym} and V_{asym} components for the samples S1 and S2.

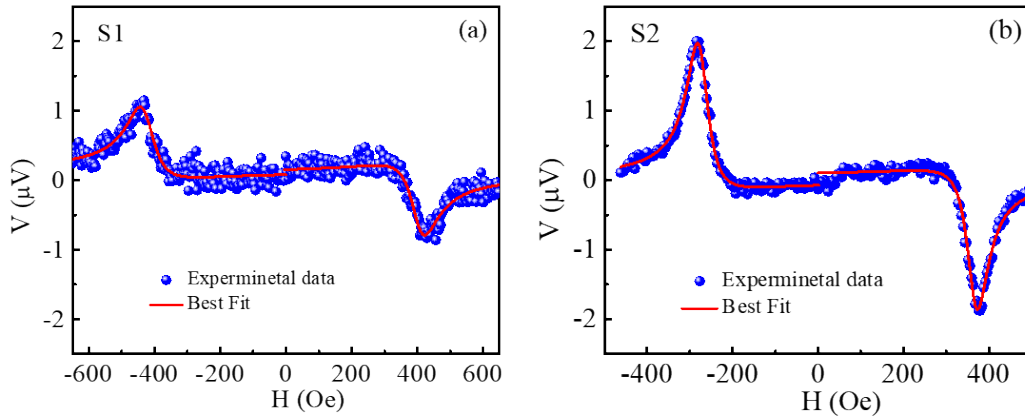


Fig. S6 ISHE measurements of the samples S1 and S2. Symbols and solid lines represent experimental data and Lorentzian fits, respectively.

Table S1 V_{sym} and V_{asym} components of the samples S1 and S2.

Sample	V_{sym} (μV)	V_{asym} (μV)
S1	0.74	0.67
S2	1.86	0.80

It can be observed that V_{sym} is much higher in sample S2 compared to S1. It indicates that spin pumping in sample S1 is blocked by MgO barrier and hence voltage decreases. If thermal effects are dominated, the strength of signal should not be decreased by 50%. Therefore, we can conclude that thermal effects are negligibly small in all the samples.

Further, intermixing may also affect the spin to charge conversion by enhancing damping constant (α). The value of α directly affects spin mixing conductance ($g_{\text{eff}}^{\uparrow\downarrow}$) and hence spin to charge conversion efficiency. In order to understand this we have prepared a new sample S3#Si/Bi₂Se₃ (10 nm)/Cu (5 nm)/CoFeB (5 nm)/TaOx (2 nm), where Cu is used due to large spin diffusion length. A 5 nm thick Cu layer can avoid any interface mixing or roughness effects on damping. It is noted here that we have chosen 10 nm Bi₂Se₃ because it shows high Bi₂Se₃ - CoFeB interface roughness (sample BB10 of the manuscript). We have performed measurements of damping properties of both the samples. Figure S7(a) and (b) show frequency dependent H_{res} and ΔH , respectively. Experimental data was fitted to the equation (4) and (6) in order to evaluate the value of α . The value of α was found to be 0.0139 ± 0.0001 . This value is much smaller than sample BB10 (0.0279 ± 0.0001). It clearly indicates that there is an interface effect which increases the value of α . Therefore, we can calculate the interface induced increase in α (α_{int}) by the following expression:

$$\alpha_{\text{int}} = \alpha(\text{BB10}) - \alpha(\text{S3}). = 0.014 \pm 0.0002$$

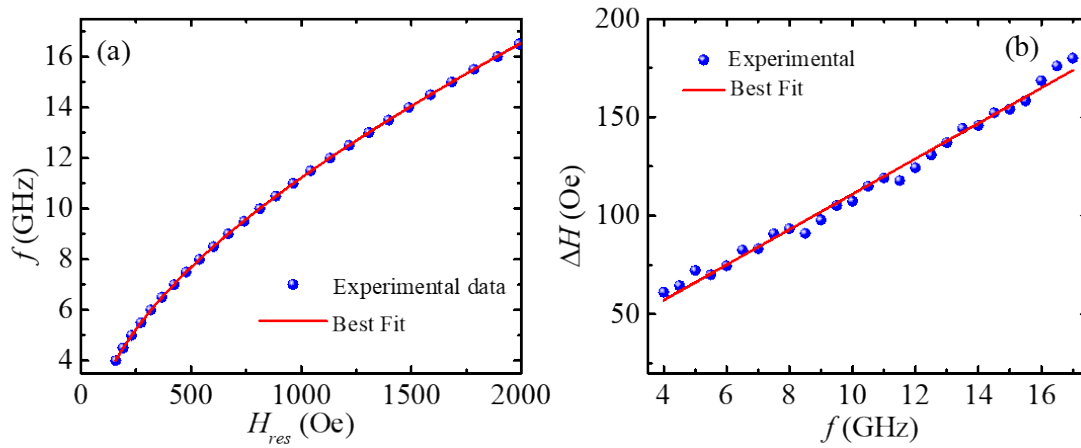


Fig. S7 f dependence of H_{res} (a) and ΔH (b) for sample S3. Solid symbols are experimental data, while solid lines are best fits using equations (4) and (6) of the manuscript in (a) and (b), respectively.

By assuming that similar nature of interface effect in all the samples, we have subtracted α_{int} from all the samples i.e. BB3- BB20.

REFERENCES

1. J. Lindner, I. Barsukov, C. Raeder, C. Hassel, O. Posth, R. Meckenstock, P. Landeros, D. L. Mills, Two-magnon damping in thin films in case of canted magnetization: Theory versus experiment. *Phys. Rev. B.* **80**, 224421 (2009).
2. X. Liu, W. Zhang, M. J. Carter, G. Xiao, Ferromagnetic resonance and damping properties of CoFeB thin films as free layers in MgO-based magnetic tunnel junctions. *Journal of Applied Physics.* **110**, 033910 (2011).
3. R. Iguchi, E. Saitoh, Measurement of Spin Pumping Voltage Separated from Extrinsic Microwave Effects. *J. Phys. Soc. Jpn.* **86**, 011003 (2016).